

The thermodynamic approach in the determination of the mechanical characteristics of materials is not new in itself. It has been used [1-5] but, in our view, has not been developed sufficiently because of imperfections of the apparatus employed. The emergence of much improved instruments in recent years for contactless temperature measurements (imaging infrared sensors, radiometers) has made it possible to turn to this problem.

This paper shows that when a specimen (component) is subjected to cyclical loading in stages, the change in its surface temperature enables us to determine the power of the heat released at the nucleation center of a fatigue crack, to calculate the change in entropy at that center, and then on the basis of the information so obtained from the experiment to predict the fatigue (endurance) limit of the object tested. Standard equipment was used to measure the temperature. This study does not go beyond the framework of the phenomenological approach.

1. Experimental Procedure. The experiment was carried out on two types of specimens: thin walled tubular specimens (Fig. 1) and prismatic cantilever specimens (Fig. 2) of St. 45 steel; the tubular specimens were subjected to longitudinal vibrations and the prismatic specimens, to flexural vibrations according to the first natural mode on a Turbo-4 vibration machine. The specimens were subjected to cyclical loads in stages with the amplitude of the vibrations growing gradually from stage to stage, starting from stresses certainly below the presumed fatigue limit and ending with stress slightly above that limit. The duration of the load in each stage was relatively short (no more than 3% of the usually accepted base of classical tests at stresses below the presumed fatigue limit or not more than 3% of the service life of the specimen at the particular stress level above the fatigue limit). At each loading stage the temperature field of the specimens was time-scanned with a Rubin MT imaging IR sensor, whose lower limit of sensitivity is 0.1°C. After each loading stage we cooled the specimen to the initial state and recorded the oscilloscope traces of its free damped vibrations, starting from the amplitudes at which the loading occurred. The results were obtained by the familiar internal-friction method [6]. A mode of free damped vibrations is achieved in a special vibration-isolated machine, adapted to measure the level of internal friction.

2. Computational Formulas. The computational scheme for a tubular specimen is shown in Fig. 3. A stress concentrator (an exactly concentric notch 0.1 mm deep) was scribed at the middle of the specimen so that when the specimen was vibrated heat would be transferred symmetrically to both ends, to which large masses (whose temperature  $T_L$  could be assumed to be constant) were attached. The surface of the tube was precision machined and then polished to eliminate random stress concentrations. Let us formulate the problem: from the temperature field  $T = T(\tau, x)$  ( $\tau$  is the time) during vibrations of the specimen with a fixed stress amplitude  $\sigma_a$  (which corresponds to each stage of stress) determine the power  $q_1 = q_1(\tau, \sigma_a)$  released in the region of the stress concentrator and the specific power  $q_2 = q_2(\tau, \sigma_a)$  released in the rest of the specimen.

For an element of the specimen we set up the heat equation with allowance for heat transfer by convection from the surface of the element (we disregard radiation because it is so small):

$$\rho c_v \partial T / \partial \tau = \kappa \partial^2 T / \partial x^2 + q_2 - r(T - T_0). \quad (2.1)$$

Here  $\rho$ ,  $c_v$ ,  $\kappa$  are the density, specific heat, and thermal conductivity of the material of the specimen  $T_0$  is the temperature of the ambient air, and  $r = \alpha \pi D / F$  ( $\alpha$  is the local convective heat transfer coefficient and  $D$  and  $F$  are the outside diameter and cross-sectional area

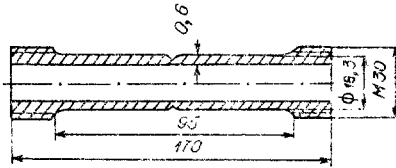


Fig. 1

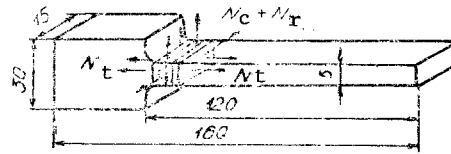


Fig. 2

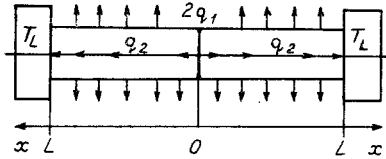


Fig. 3

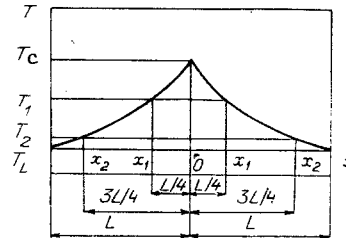


Fig. 4

of the specimen). In Eq. (2.1) the temperature is assumed to be constant over the thickness of the tube since it is a thin-walled tube.

Our experiment showed that after some time  $\tau_0$  the temperature field of the specimen becomes virtually stabilized in each loading stage; accordingly, we can consider the process to be quasistationary, i.e.,  $\partial T/\partial \tau \approx 0$  (at  $\tau > \tau_0$ ). In this case Eq. (2.1) becomes

$$\partial^2 T/\partial x^2 - rT/\kappa = -rT_0/\kappa - q_2/\kappa. \quad (2.2)$$

The general solution of the inhomogeneous equation (2.2) is

$$T = C_1 \exp(x\sqrt{r/\kappa}) + C_2 \exp(-x\sqrt{r/\kappa}) + T_0 + q_2/r.$$

After finding the constants of integration  $C_1$  and  $C_2$  from the boundary conditions  $\partial T/\partial x = -q_1/(\kappa F)$  at  $x = 0$  and  $T = T_L$ , at  $x = L$  we obtain the law of temperature distribution along the axis of the specimen:

$$T = T_L X + (T_0 + q_2/r)(1 - X) + q_1 [X \exp(\lambda L) - \exp(\lambda x)] / (F\sqrt{r\kappa}) \quad (2.3)$$

$$(X = \cosh(\lambda x)/\cosh(\lambda L), \lambda = \sqrt{r/\kappa}).$$

In the case of the prismatic specimens subjected to flexural vibrations we solved the following problem: at each stage of the loading calculate the damaging power  $N_d$  released in the presumed center of accumulation of fatigue defects, which in all 20 specimens tested, as recorded by an imaging IR sensor, was located in the region of the grip (this zone is shaded in Fig. 2).

The calculation was carried out from the equation of power balance

$$N_d = N - N_h - N_t - N_c - N_r. \quad (2.4)$$

where  $N$  is the total power dissipated through internal friction of the material at the crack center,  $N_h$  is the power expended to heat the crack center, and  $N_t$ ,  $N_c$ , and  $N_r$  are the powers of the heat removed from the crack center by thermal conduction, convection, and radiation, respectively.

We determined the total power  $N$  from the internal friction parameters  $\gamma$  and  $\beta$  of the material, which were calculated from the oscilloscope traces (recorded after each stage of loading) of the free damped vibrations of the specimens, using the formula [7]

$$N = \frac{\beta V E f}{2(\gamma + 3)} \left( \frac{\sigma_a}{E} \right)^{\gamma+2}$$

( $V$  is the volume of the presumed crack center,  $f$  is the vibration frequency of the specimen,  $\sigma_a$  is the maximum stress amplitude at the crack center, and  $E$  is Young's modulus of the material). Using well known formulas [8], we calculated  $N_h$ ,  $N_t$ ,  $N_c$ , and  $N_r$ .

**3. Results.** Ten tubular specimens were tested by the procedure described above. In the typical thermal diagram of  $T = T(x)$  along the axis of the specimen shown in Fig. 4 we clearly see an internal heat source  $q_1$  in the region of a stress concentrator with tempera-

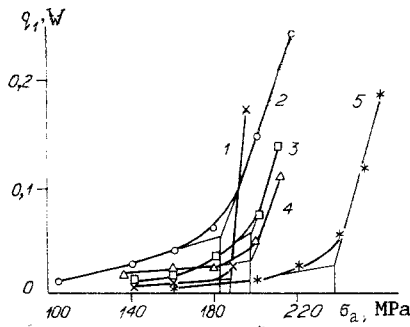


Fig. 5

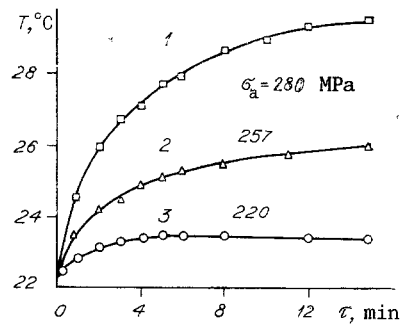


Fig. 6

ture  $T_C$ . Such diagrams were recorded at 1-min intervals at all loading stages. The values of  $q_1$  and  $q_2$  were determined by processing the experimental graphs of  $T = T(x)$  (Fig. 4) by the method of least squares [9] with the assumption that temperature is distributed along the axis of the specimen in accordance with law (2.3). The values of  $T_C$ ,  $T_1$ ,  $T_2$ , and  $T_L$  from the graphs  $T = T(x)$  were taken at four points with coordinates  $x_0 = 0$ ,  $x_1 = L/4$ ,  $x_2 = 3L/4$ , and  $x_L = L$ . For example, the parameter  $q_1$  was calculated to within 5% with a confidence coefficient of 0.95. It turned out that  $q_1$  is virtually independent of the time  $\tau$  ( $\tau > \tau_0$ ) when the calculation was made in the given stage and depends only on the amplitude  $\sigma_a$  of the cyclical stress, i.e.,  $q_1 = q_1(\sigma_a)$ . The calculation was carried out at  $\rho = 7800 \text{ kg/m}^3$ ,  $c_V = 662 \text{ J/(kg} \times \text{K)}$ ,  $\kappa = 38 \text{ W/(m} \times \text{K)}$ ,  $\alpha = 23.2 \text{ W/(m}^2 \times \text{K)}$ ,  $D = 18.3 \text{ mm}$ ,  $F = 33.4 \text{ mm}^2$ ,  $L = 47.5 \text{ mm}$ .

The graphs of  $q_1 = q_1(\sigma_a)$  in Fig. 5 were plotted for five specimens (curves 1-5). All the graphs have kinks, whose abscissas can be treated as the individual endurance limits of the specimens. This follows from the fact that the endurance limits so determined virtually coincided with the values calculated by other methods (see Table 1).

For the prismatic specimens we plotted graphs of the time variation of the temperature of the fatigue-crack initiation center at each stage of the loading. Figure 6 shows typical graphs for one specimen, from which we see that when the specimens are loaded with stresses below the fatigue limit ( $\sigma_a < \sigma_{-1}$ ), the temperature of the crack center becomes stabilized some time after loading begins (curve 3) but temperature stabilization does not occur (curves 1 and 2) when the stresses exceed the fatigue limit ( $\sigma_a > \sigma_{-1}$ ). This result correlates with previous studies (see, e.g., [10]) and also allows the individual fatigue limit of the specimen to be determined from the temperature field kinetics; for the tested specimen the fatigue limit lies in the range  $\sigma = 220\text{--}257 \text{ MPa}$  ( $\sigma_{-1} = 232 \text{ MPa}$  for this specimen by the internal-friction method). If the accuracy with which  $\sigma_{-1}$  is determined by this method is to be increased the degree of change in load must be decreased as the presumed fatigue limit of the specimen is approached.

The Eq. (2.4) was used to calculate  $N_d$  (the power expended on the development of fatigue damage) at different points of the curve  $T = T(\tau)$  at all stages of specimen loading. An important result was obtained: calculation of  $N_d$  on any part of the curves  $T = T(\tau)$  showed that  $N_d \approx 0$  when the specimens are loaded with stresses below the fatigue limit ( $\sigma_a < \sigma_{-1}$ ) while when the load on the specimens is higher than the fatigue limit ( $\sigma_a > \sigma_{-1}$ ) we have that  $N_d > 0$  and, interestingly, depends only on  $\sigma_a$  and not on the point for which the calculation was made, i.e.,  $N_d \approx \text{const}$ .

The fact that  $N_d$  is constant in the respective stages of loading of the specimens above the fatigue limit (at  $\sigma_a > \sigma_{-1}$ ) gives reason to assume that  $N_d$  is an individual characteristic of the specimen, thus opening up prospects for predicting the service life of the machine component. As shown in [2], the damaging energy  $E_d$  does not depend on the level of stresses in the material and in essence is a characteristic of the material; therefore, knowing  $E_d$  for a given material and determining  $N_d$  at the level of stresses corresponding to the actual operating conditions of the machine component, we can obtain a formula for its service life:  $\tau = E_d/N_d$ .

4. Entropy Approach to the Determination of the Fatigue Limit. The literature has reported attempts to use the "entropy" approach to the description of the fracture process and, in particular, the process of fatigue damage buildup [3, 5, 11]. Indeed, taking the expression for the increment in specific entropy of an isolated particle of the body under consideration [12]

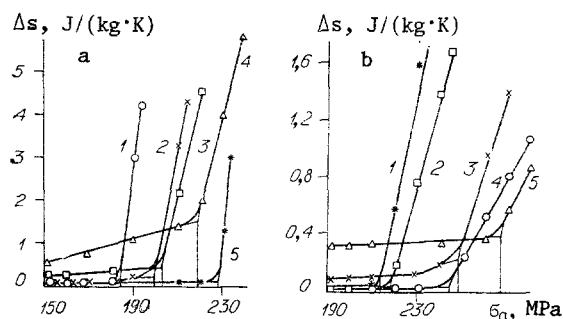


Fig. 7

TABLE 1

Sample No.	Experiment							
	with longitudinal vibrations					with flexural vibrations		
	$\sigma_{-1}$ , MPa (by the internal-friction method)	$\sigma_{-1}^*$ , MPa [from the graph $\Delta s = \Delta s(\sigma_a)$ ]	$\sigma_{-1}^{**}$ , MPa [from the graph $q_1 = q_1(\sigma_a)$ ]	,100, %		$\sigma_{-1}$ , MPa (by the internal-friction method)	$\sigma_{-1}^*$ , MPa [from the graph $\Delta s = \Delta s(\sigma_a)$ ]	,100, %
				$\frac{\sigma_{-1}^* - \sigma_{-1}}{\sigma_{-1}}$	$\frac{\sigma_{-1}^{**} - \sigma_{-1}}{\sigma_{-1}}$			$\frac{\sigma_{-1}^* - \sigma_{-1}}{\sigma_{-1}}$
1	195	200	187	2,56	4,1	244	248	1,62
2	180	184	182	2,22	1,11	232	243	4,73
3	200	202	198	1	1	210	218	3,8
4	210	218	198	3,81	5,7	268	265	1,12
5	220	228	237	3,64	7,73	207	212	2,42

$$ds = (c_v/T)dT, \quad (4.1)$$

we integrate it as the particle passes from state 1 to state 2:

$$\Delta s = s_1 - s_2 = c_v \ln (T_2/T_1). \quad (4.2)$$

Equation (4.2) provides a practical way of determining the change in the specific entropy of an observed point of an operating component from the increment in the temperature of that point and determining the fatigue limit of the component from the change in entropy. For this purpose we must apply a cyclical load to the specimen (component) in stages, with the stress amplitude  $\sigma_a$  increasing from stage to stage, and at every stage of the loading we must also take two readings  $T_1$  and  $T_2$  (after a certain interval  $\Delta\tau$ ) of the temperature of some point of the component, located as close as possible to a crack center, use Eq. (4.2) at each stage to calculate the entropy change  $\Delta s$ , and then plot the graph  $\Delta s = \Delta s(\sigma_a)$ ; as shown by experiment, this graph has a distinct kink, whose abscissa is the individual fatigue limit of the component tested.

This method was used to process the experiments described above with longitudinal (a) and flexural (b) vibrations of the specimens (Fig. 7). We see that in all the specimens the change  $\Delta s$  is insignificant up to the fatigue limit and after that increases abruptly; the kink in  $\Delta s = \Delta s(\sigma_a)$  is more characteristic than in the corresponding graphs of the absorption coefficient  $\psi = \psi(\sigma_a)$ , from which  $\sigma_{-1}$  is determined by the internal-friction method [6], and in the graphs  $q_1 = q_1(\sigma_a)$  (see Fig. 5). This permits the conclusion that  $\Delta s$  is an even more sensitive parameter of the structural changes occurring in the component than is such a structure-sensitive parameter as  $\psi$ . The method of determining the fatigue limit from the entropy change, therefore, is very promising besides being nondestructive. In order to implement this method in practice it is sufficient to monitor the temperature of the presumed crack center at different loading stages, using standard equipment, an imaging IR sensor or radiometer, which is sufficiently sensitive to obtain correct results.

The change  $\Delta s$  can be written as  $\Delta s = \Delta s_s + \Delta s_d$ , where  $\Delta s_s$  is the safe part of  $\Delta s$  dissipated into the surrounding medium and  $\Delta s_d$  is that part of  $\Delta s$  expended on the development and buildup of fatigue damage. Clearly, when specimens are loaded to the fatigue limit  $\Delta s =$

$\Delta s_s$  ( $\Delta s_d = 0$ ) and beyond it, i.e.,  $\Delta s_d > 0$ , where  $\Delta s_d > \Delta s_s$ , and this inequality is stronger when the loading takes place at a higher stress level.

Table 1 compares the fatigue limit determined in different ways for five specimens under longitudinal and flexural vibrations. Comparison of the results obtained by the thermal methods described above with the results with the internal-friction method, which can be considered fairly well developed [6], shows the discrepancies are small (maximum of 7.73%) and that calculation from the entropy change gives slightly smaller deviations.

#### LITERATURE CITED

1. V. Ya. Bash, Thermoelectric Studies of Stresses and Strains [in Russian], Naukova Dumka, Kiev (1984).
2. S. E. Gurevich and A. P. Gaevoi, "Procedure for the experimental determination of the failure energy under cyclical loading," *Zavod. Lab.*, No. 9 (1973).
3. I. I. Novikov, "Thermodynamic aspects of plastic deformation and fracture of metals," in: *Physicomechanical and Thermophysical Properties of Metals* [in Russian], Nauka, Moscow (1976).
4. V. T. Troshchenko, Deformation and Fracture of Metals under Multiple-Cycle Loading [in Russian], Naukova Dumka, Kiev (1981).
5. V. V. Fedorov, Thermodynamic Aspects of the Strength and Fracture of Solids [in Russian], Fan, Tashkent (1979).
6. I. Ya. Shpigel'burd, G. A. Kurilenko, and V. G. Atapin, "Testing the fatigue strength of machine components by the internal-friction method under production conditions," in: *Energy Scattering During Vibrations of Mechanical Systems* [in Russian], Naukova Dumka, Kiev (1982).
7. I. Ya. Shpigel'burd, G. A. Kurilenko, A. A. Zhidkov, et al., "Evaluation of the damageability of carbon steel under cyclical loads on the basis of temperature-field measurement," in: *Energy Scattering During Vibrations of Mechanical Systems* [in Russian], Naukova Dumka, Kiev (1985).
8. S. S. Kutateladze and V. M. Borishanskii, *Handbook of Heat Transfer* [in Russian], Gosénergoizdat, Moscow-Leningrad (1959).
9. Yu. V. Linnik, *Method of Least Squares and the Fundamentals of the Theory of Processing of Observations* [in Russian], Fizmatgiz, Moscow (1962).
10. L. A. Glikman and V. P. Tekht, "On the physical nature of metal fatigue," in: *Some Problems of the Fatigue Strength of Steel* [in Russian], Mashgiz, Moscow-Leningrad (1953).
11. D. A. Kiyalbaev and A. I. Chudnovskii, "On the fracture of deformable materials," *Prikl. Mekh. Tekh. Fiz.*, No. 3 (1970).
12. E. Fermi, *Thermodynamics*, Prentice-Hall, Englewood Cliffs, N.J. (1973).